lated from the formula:

$$[Ca^{2+}] = K_D(F_0/F_s)(R - R_{min})/(R_{max} - R)$$

where the dissociation constant $K_D = 225 \times 10^{-9} M$, $F_0/F_s = 7.5$, $R_{min} = 0.47$, $R_{max} = 11.7$, and R is the ratio of the measured fluorescence excited by 340- and 380-nm light. Numerical values reported are an average of at least 32 adjacent pixels. Exposure time for each picture was 250 or 500 msec. Cells were exposed to ultraviolet light only during collection periods, less than 30 seconds for any one cell. Bleaching was less than 2%. Data acquisition for a 140 × 240 pixel image required approximately 1.5 seconds and was always begun at the end of a stimulus pulse. Because of the long acquisition time, we underestimate the peak amplitude of the Ca^{2+} changes resulting from the application of agonists.

8. G. Grynkiewicz, M. Poenie, R. Y. Tsien, *J. Biol. Chem.* **260**, 3440 (1985); D. A. Williams, K. E. Fogarty, R. Y. Tsien, F. S. Fay, *Nature (London)* **318**, 558 (1985); R. Y. Tsien and M. Poenie, *Trends Biochem. Sci.* **11**, 450 (1986); J. A. Connor, *Proc. Natl. Acad. Sci. U.S.A.* **83**, 6179 (1986); ———, M. C. Cornwall, G. H. Williams, *J. Biol. Chem.* **262**, 2919 (1987); C. Cohan, J. A. Connor, S. B. Kater, *J. Neurosci.* **7**, 3588 (1987).
9. R. E. Numann and R. K. S. Wong, *Neurosci. Lett.* **47**, 289 (1984); A. R. Kay, R. Miles, R. K. S. Wong, *J. Neurosci.* **6**, 2915 (1986); R. E. Numann, W. J. Wadman, R. K. S. Wong, *J. Physiol. (London)* **393**, 331 (1987); A. R. Kay and R. K. S. Wong, *ibid.* **392**, 603 (1987).

10. In a separate, control series of experiments, 19 cell preparations from six animals were observed for periods of 1 to 1.5 hours after dissociation. The 96 neurons in this group had a mean unstimulated $[Ca^{2+}]$ of 80 nM. Of these neurons, 70% held their $[Ca^{2+}]$ constant to within 15% during 30 to 40 minutes of observations by microscopy. The rest underwent much larger increases during the observation period, but fewer than 5% of the neurons showed rapid, spontaneous Ca^{2+} increases.
11. In experiments without TTX, the initial application of agonist nearly always caused a runaway response; the cells went to conditions where internal $[Ca^{2+}]$ exceeded 300 nM in a period of several minutes. The magnitude of the primary Ca^{2+} change was also systematically larger than the responses shown in Fig. 1. This instability is not surprising given that the isolated cells have been stripped of all inhibitory inputs. Bath application of GABA greatly dampened the responses to glutamate.

12. Y. A. Hannun, C. R. Loomis, A. H. Merrill, R. M. Bell, *J. Biol. Chem.* **261**, 12604 (1986); E. Wilson, M. C. Olcott, R. M. Bell, A. H. Merrill, J. D. Lambeth, *ibid.*, p. 12616.

13. High K^+ saline was applied with the center of the flow pattern on the soma. Experiments were designed to maximize the dendrite-soma gradients of Ca^{2+} by making the influx period brief. That is, even if one assumes a uniform influx of Ca^{2+} in the soma and dendrite, one expects a larger transient change in the dendrite than in the soma from surface to volume considerations. This difference decreased with longer stimuli as the cytoplasmic buffers saturated in the soma. Where the high K^+ stimulus was applied for more than 10 seconds, the dendritic soma Ca^{2+} difference was never more than 20 to 30 nM at a high mean level.
14. Measured gradients of Ca^{2+} have been used to compute the associated flux down the dendrite given that there are no longitudinal barriers. The three fluxes of importance, free Ca (Ca^{2+}), Ca bound to indicator (CaI), and Ca bound to mobile cell buffers (CaB), were computed from the integrated form of Fick's law using the following parameters: the diffusion coefficient $D_{Ca} = 6 \times 10^{-6}$ cm^2/sec; mean dendrite diameter = 4 μm; fura-2 concentration = 300 μM; $K_D = 225$ nM; diffusion coefficient of CaI = 2×10^{-6}; intrinsic buffer concentration = 250 μM with $K_D = 1$ μM; Ca^{2+} gradient of 250 to 150 nM over 20-μm distance. The three components sum to approximately 1 pA, and from this we make two observations. First, this flux could be supplied by a small number of channels. Second, it is unlikely that internal stores could supply the Ca^{2+} required to maintain the gradient. A current of 1 pA over a 5-minute period involves the movement of 1.5×10^{-15} mol of $[Ca^{2+}]$ from the distal 10 to 15 μm of the dendrite in our preparations (~50 fl volume). Even if all of this volume were internal store, Ca^{2+} would have to be 30 mM, an enormous level, in order to support the gradient. Furthermore, this store would be inaccessible to fura-2 since the indicator reports submicromolar $[Ca^{2+}]$ in unstimulated dendrites.

15. H. Reuter, *Nature (London)* **301**, 569 (1983); R. W. Tsien *et al.*, *J. Mol. Cell. Cardiol.* **18**, 691 (1986); D. Armstrong and R. Eckert, *Proc. Natl. Acad. Sci. U.S.A.*, **84**, 2518 (1987); S. A. DeRiemer, J. A. Strong, K. A. Albert, P. Greengard, L. K. Kaczmarek, *Nature (London)* **313**, 313 (1985); J. A. Strong, A. P. Fox, R. W. Tsien, L. K. Kaczmarek, *ibid.* **325**, 714 (1987).
16. R. C. Malenka, D. V. Madison, R. Andrade, R. A. Nicoll, *J. Neurosci.* **6**, 475 (1986).
17. L. Coussens, L. Rhee, P. Parker, A. Ullrich, *DNA (N.Y.)* **6**, 389 (1987).
18. R. K. S. Wong, D. A. Prince, A. I. Basbaum, *Proc. Natl. Acad. Sci. U.S.A.* **76**, 986 (1979); P. A. Schwartzkroin and M. Slawsky, *Brain Res.* **135**, 157 (1977).
19. T. V. P. Bliss, R. M. Douglas, M. L. Errington, M. A. Lynch, *J. Physiol. (London)* **377**, 391 (1986); K. G. Bainbridge and J. Miller *Brain Res.* **221**, 299 (1981); G. Lynch and M. Baudry, *Science* **224**, 1057 (1984).

20. Research funded by AT&T Bell Labs, the Air Force Office of Scientific Research contract F49620 (J.A.C.), NATO Science Fellowship from the Netherlands Organization for the Advancement of Pure Research (W.J.W.), and NIH grant NS24519 (R.K.S.W.).

11 December 1987; accepted 7 March 1988

Highly Cooperative Opening of Calcium Channels by Inositol 1,4,5-Trisphosphate

TOBIAS MEYER, DAVID HOLOWKA,* LUBERT STRYER

The kinetics of calcium release by inositol 1,4,5-trisphosphate (IP_3) in permeabilized rat basophilic leukemia cells were studied to obtain insight into the molecular mechanism of action of this intracellular messenger of the phosphoinositide cascade. Calcium release from intracellular storage sites was monitored with fura-2, a fluorescent indicator. The dependence of the rate of calcium release on the concentration of added IP_3 in the 4 to 40 nM range showed that channel opening requires the binding of at least three molecules of IP_3. Channel opening occurred in the absence of added adenosine triphosphate, indicating that IP_3 acts directly on the channel or on a protein that gates it. The channels were opened by IP_3 in less than 4 seconds. The highly cooperative opening of calcium channels by nanomolar concentrations of IP_3 enables cells to detect and amplify very small changes in the concentration of this messenger in response to hormonal, sensory, and growth control stimuli.

THE PHOSPHOINOSITIDE CASCADE plays a central role in the transduction of many hormonal, sensory, and growth control stimuli (*1*). Hydrolysis of phosphatidylinositol 4,5-bisphosphate by a receptor-triggered phospholipase C generates two intracellular messengers, 1,4,5-trisphosphate (IP_3) and diacylglycerol. IP_3 raises the cytosolic level of calcium ion by releasing it from the endoplasmic reticulum (*2*). High-affinity binding sites for IP_3 have been detected in permeabilized cells (*3*) and microsomal membrane preparations (*4*). The effectiveness of IP_3 in releasing Ca^{2+} in the absence of adenosine triphosphate (ATP) or other high-potential phosphoryl donors has suggested that IP_3 directly activates a Ca^{2+}-selective channel (*5*).

We have investigated the kinetics of IP_3-induced Ca^{2+} release from intracellular storage pools in permeabilized rat basophilic leukemia (RBL) cells (*6*) to gain insight into the molecular mechanism of action of IP_3. The antigen-mediated cross-linking of immunoglobulin E (IgE)–receptor complexes on the surface of RBL cells leads to the formation of IP_3 (*7*). The consequent rise in the cytosolic Ca^{2+} (*8*) contributes to the exocytic release of histamine and other mediators. RBL cells from the 2H3 subline (*9*) were harvested (*10*), washed by centrifugation, and resuspended in a buffered salt solution without added divalent cations (135 mM NaCl, 5 mM KCl, and 20 mM Hepes, *p*H 7.4). After three washes, 2×10^6 cells per milliliter were resuspended in an ice-cold, high ionic strength KCl buffer (140 mM KCl, and 30 mM Hepes, *p*H 7.4) that contained 1.5 μM fura-2 (Molecular Probes), a fluorescent Ca^{2+} indicator (*11*). Buffers containing fura-2 and all inositides were passed through a chelating column (diphenylenediaminepentacetic acid coupled to ω-aminobutyl agarose) to lower the total Ca^{2+} concentration and that of heavy metal ions to less than 100 nM. The plasma membrane of the RBL cells was permeabilized by incubating them in KCl

Department of Cell Biology, Sherman Fairchild Center, Stanford University School of Medicine, Stanford, CA 94305.

*On sabbatical leave from the Department of Chemistry, Baker Laboratory, Cornell University, Ithaca, NY 14853.

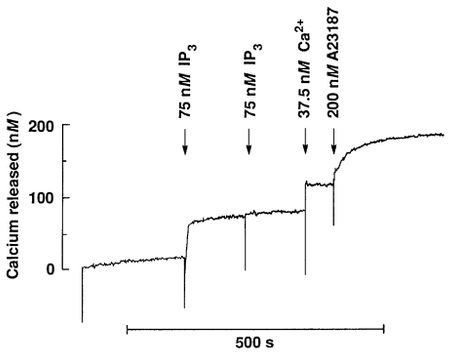

Fig. 1. Time course of changes in $[Ca^{2+}]_s$ in a typical experiment with permeabilized RBL cells at 11°C. The addition of 75 n*M* IP_3 (3 μl of a 50-μ*M* solution) to a 2-ml suspension of stirred, saponin-permeabilized cells fully depleted the IP_3-releasable Ca^{2+} store. The amount of Ca^{2+} in IP_3-insensitive stores was determined by the addition of the Ca^{2+} ionophore A23187 (2 μl of a 200-μ*M* solution in ethanol). Only 10% of the increase in fluorescence came from the added A23187. The downward deflection marker spikes were obtained by interrupting the excitation beam with the tip of the pipette during injection. The mixing time was less than 2 seconds. The free Ca^{2+} concentration was of the order of 0.1 μ*M* in all experiments. A total of Ca^{2+} release of 50 n*M* increased *f* from about 0.31 to 0.34.

buffer containing saponin (40 μg/ml) (Sigma) for 10 to 15 minutes at room temperature. Permeabilization was monitored by the uptake of trypan blue. When more than 80% of the cells were permeabilized, aliquots of the suspension were transferred to acrylic cuvettes (Sarstedt), cooled to 11°C in a water bath, and used within 30 minutes (*12*).

Measurements of fluorescence were carried out with an SLM 8000 spectrofluorimeter. The system was calibrated with fura-2 in KCl buffer containing 2 m*M* EGTA or 10 m*M* $CaCl_2$ (*11*). The initial concentration of fura-2 and the fraction of fura-2 containing bound Ca^{2+} in the permeabilized cell suspension were determined by fluorescence (excitation, 340 and 370 nm; emission, 510 nm). The kinetics of Ca^{2+} efflux from intracellular stores of RBL cells were determined by monitoring the increase in fluorescence intensity obtained on excitation at 340 nm. The concentration of unbound Ca^{2+} ($[Ca^{2+}]_u$) is given by

$$[Ca^{2+}]_u = K_d f/(1 - f)$$

where K_d is the dissociation constant of the Ca^{2+}–fura-2 complex (220 n*M*) (*11*), and *f* is the fraction of fura-2 containing bound Ca^{2+}. $[Ca^{2+}]_s$, the sum of the concentrations of free Ca^{2+} and Ca^{2+} complexed to fura-2, is given by

$$[Ca^{2+}]_s = [Ca^{2+}]_u + f[\text{fura-2}]$$

$[Ca^{2+}]_s$ is nearly equal to the total concentration of released Ca^{2+} because of neglible buffering by components other than fura-2, as evidenced by the finding that the fluorescence change obtained on addition of a known amount of Ca^{2+} matched that calculated for binding to fura-2 alone (*13*).

IP_3 (75 n*M*) induced a rapid rise in free Ca^{2+} (Fig. 1). There was no further increase after the addition of a second aliquot of IP_3. Our experiments were carried out in the absence of added Mg^{2+} and ATP to prevent refilling of Ca^{2+} stores by an ATP-driven Ca^{2+} pump (*14*). A known amount of Ca^{2+} was then added to check the calibration of the Ca^{2+} release scale. Finally, A23187 (Sigma), a Ca^{2+} ionophore, was added to release Ca^{2+} from compartments unaffected by IP_3. In most experiments, IP_3 released between 30 and 70% of the total sequestered Ca^{2+}. For an intracellular volume of 1 μl per 10^6 cells (*15*), release of this IP_3-sensitive pool would raise the cytosolic Ca^{2+} level from 0.1 μ*M* in unstimulated cells (*8*) to more than 20 μ*M* (in the absence of buffering) in fully stimulated cells. The rate of Ca^{2+} release changed by less than a factor of 3 in the temperature range from 4° to 35°C. Nearly all of the IP_3-sensitive pool could be released within a minute by the addition of as little as 20 n*M* IP_3. The same concentration of inositol 1,3,4,5-tetrakisphosphate (Calbiochem) or inositol 1:2-cyclic 4,5-trisphosphate (from P. Majerus) did not cause measurable release of Ca^{2+}. No change in bulk Ca^{2+} was observed after the addition of IP_3 to a suspension of unpermeabilized cells.

[^{3}H]IP_3 (NEN) (5 to 50 n*M*) was added to permeabilized cells to determine whether IP_3 was hydrolyzed to an appreciable extent in the course of a Ca^{2+}-release experiment. No detectable hydrolysis occurred in 10 minutes, as monitored by anion-exchange high-pressure liquid chromatography. Hydrolysis was minimal because of the absence of Mg^{2+} in the buffers used in the release experiments (*16*). Preliminary binding studies showed that the concentration of high-affinity binding sites for IP_3 was less than 0.2 n*M* (*17*). Thus, the free concentration of IP_3 was nearly equal to the concentration of added IP_3 throughout the course of efflux experiments.

The rate of release of Ca^{2+} increased with increasing concentration (3 to 150 n*M*) of IP_3 (Fig. 2). The extent of Ca^{2+} release elicited by IP_3 concentrations greater than 20 n*M* reached a saturating level within 30 seconds after addition (*18*). At the lowest IP_3 concentrations (<10 n*M*), the extent of Ca^{2+} release at long times was sometimes less than attained with higher concentrations of IP_3, possibly because residual Mg^{2+}-ATP in the permeabilized cells powered the refilling of Ca^{2+} stores.

The smooth lines in Fig. 2 are nonlinear

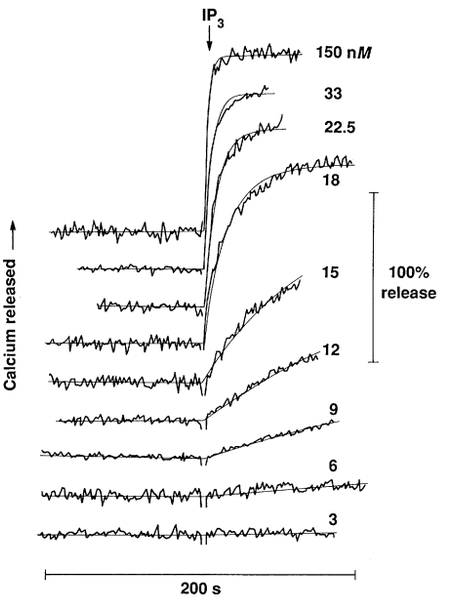

Fig. 2. Time course of Ca^{2+} efflux by a range of concentrations of added IP_3 in a series of experiments. The data were obtained as in Fig. 1 and were corrected for injection spike artifacts and for baseline drift. A second aliquot of 100 n*M* IP_3 was added after 100 seconds to determine the total amount of IP_3-releasable stored Ca^{2+} so that the data could be normalized to the same scale. The change in *f* in these experiments ranged from 0.02 to 0.03, ensuring a nearly linear relation between *f* and the amount of Ca^{2+} released.

least-square fits of the data to single-exponential rises of the form

$$f(t) = [f(c) - f(0)]\,[1 - \exp(-k_{obs}t)]$$

in which $f(t)$ is the fraction of fura-2 containing bound Ca^{2+} at time *t*, $f(0)$ is the fraction before the addition of IP_3, $f(c)$ is the fraction after complete release of the IP_3-sensitive pool, and k_{obs} is the observed first-order rate constant for IP_3-induced efflux of Ca^{2+}. In these experiments, $f(t)$ is nearly proportional to $[Ca^{2+}]_s$. The good fit of the efflux data to single-exponential decays implies that the efflux rate is proportional to the concentration of Ca^{2+} in the IP_3-sensitive pool and is consistent with the passive efflux of Ca^{2+} through channels. The absence of a detectable lag between the addition of IP_3 and the onset of an initially constant efflux rate indicates that the Ca^{2+} channels bind IP_3 and open in less than 4 seconds.

A plot of the logarithm of k_{obs} versus the logarithm of IP_3 concentration is shown in Fig. 3. The slope of this log-log plot, determined from rates observed for IP_3 concentrations ranging between 4 and 40 n*M*, is 2.7 ± 0.2 (SD). The points for concentrations of IP_3 greater than 50 n*M* deviate from linearity. It remains to be determined whether this deviation is a consequence of the mixing time in our experiments, diffu-

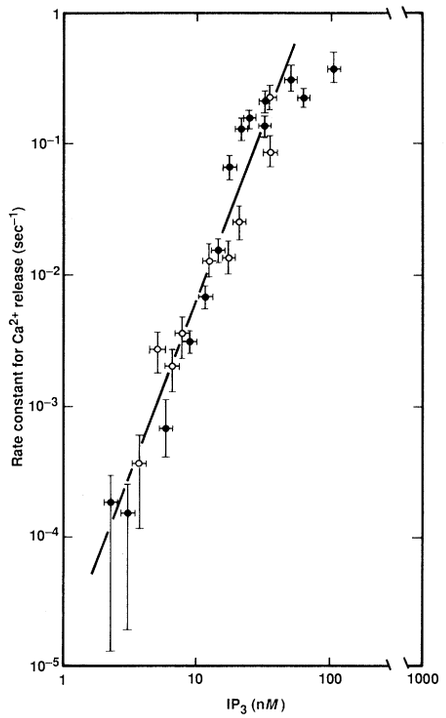

Fig. 3. Values of k_{obs} obtained from the best fits shown in Fig. 2 (●) and from another data set (○) are plotted as a function of IP_3. Error bars in the horizontal direction correspond to the estimated uncertainty in the concentration of IP_3; those in the vertical direction reflect the uncertainty in the best fit values for k_{obs}. The solid line is the least-squares fit to a straight line for values of concentrations of IP_3 ranging from 4 to 40 nM.

sion limitations in the permeabilized cells, or an approach to a limiting efflux rate. It seems likely that k_{obs} is proportional to the fraction p of open channels for concentrations of IP_3 less than 50 nM. The slope of 2.7 ± 0.2 then indicates that opening of a Ca^{2+} channel requires the binding of at least three molecules of IP_3 (*19*). Ca^{2+}-induced Ca^{2+} release (*20*) probably did not contribute significantly to this high degree of cooperativity; release of the entire IP_3-sensitive store increased the concentration of free Ca^{2+} from 0.1 to only 0.11 μM.

The experimental data can be fit to a simple model in which the independent binding of three molecules of IP_3 to the closed state of the channel (C) is followed by a rapid intramolecular transition to the open form (O).

$$C_0 \underset{k_-}{\overset{3k_+L}{\rightleftharpoons}} C_1 \underset{2k_-}{\overset{2k_+L}{\rightleftharpoons}} C_2 \underset{3k_-}{\overset{k_+L}{\rightleftharpoons}} C_3 \underset{k_2}{\overset{k_1}{\rightleftharpoons}} O_3$$

In this minimal scheme, k_+ and k_- are the forward and reverse rate constants for the binding of IP_3 to a site on the channel (or on a protein that gates the channel), and k_1 and k_2 are the rates of channel opening and closing, respectively. The fraction p of channels open at a given concentration L of IP_3 is

$$p(L) = \frac{(L/K_d)^3 K_c}{(1 + L/K_d)^3 + (L/K_d)K_c}$$

where $K_d = k_-/k_+$ and $K_c = k_1/k_2$. In this model, channel opening is highly cooperative, whereas IP_3 binding is noncooperative or weakly cooperative for $K_c < 100$, in agreement with previous findings (*3, 4*). The experimental data do not suffice to define the values of these rate or equilibrium constants. However, they do place constraints on allowable values. The absence of a detectable lag in efflux (on the time scale of 4 seconds) indicates that

$$(k_+L + k_-) > 0.25 \text{ sec}^{-1} \text{ and}$$
$$(k_1 + k_2) > 0.25 \text{ sec}^{-1}$$

Calculated plots of log p versus log L over a wide range of values of K_c are nearly linear and have a slope greater than 2.5 for $L < K_d$. The experimental data (Fig. 3) obey these criteria for L less than 35 nM. Hence, K_d must be greater than 35 nM. This constraint, taken together with the kinetic one noted above, implies that k_- is greater than about 0.25 sec^{-1} (*21*). Kinetic studies of IP_3-induced channel opening in times of milliseconds are needed to test this minimal model. Such information could be obtained by rapid addition of IP_3 to microsomal vesicles loaded with Ca^{2+}. Laser-induced photolysis of caged analogs of IP_3 (*22*) would be another means of generating a rapid increase in the concentration of this agonist.

The highly cooperative opening of Ca^{2+} channels by nanomolar concentrations of IP_3 enables cells to detect and amplify very small increases in the concentration of this messenger molecule. Furthermore, the channels are designed to be opened and closed on the time scale of seconds or less. Hence, large changes in the concentration of Ca^{2+} in the cytoplasm can be rapidly achieved. Indeed, rapid oscillations and spiking of cytoplasmic Ca^{2+} concentrations have been observed in a variety of stimulated cells (*23*). The high degree of cooperativity of IP_3-induced channel opening makes possible these repetitive bursts of Ca^{2+} (*24*). The concerted opening of the IP_3-gated channel exemplifies a recurring motif, the construction of ion channels from multiple subunits (*25*).

REFERENCES AND NOTES

1. L. E. Hokin, *Annu. Rev. Biochem.* **54**, 205 (1985); M. J. Berridge and R. F. Irvine, *Nature* **312**, 315 (1984).
2. H. Streb, J. P. Heskop, R. F. Irvine, D. Schulz, M. J. Berridge, *J. Biol. Chem.* **260**, 7309 (1985); M. J. Berridge, *Annu. Rev. Biochem.* **56**, 159 (1987); J. W. Putney, Jr., *Am. J. Physiol.* **252**, 149 (1987).
3. A. Spät, P. G. Bradford, J. S. McKinney, R. P. Rubin, J. W. Putney, Jr., *Nature* **319**, 514 (1986).
4. A. Spät, A. Fabiato, R. P. Rubin, *Biochem. J.* **233**, 929 (1986); P. F. Worley, J. M. Baraban, S. Supattapone, V. S. Wilson, S. H. Snyder, *J. Biol. Chem.* **262**, 12132, (1987); G. Guillemette, T. Balla, A. J. Baukal, K. J. Catt, *Proc. Natl. Acad. Sci. U.S.A.* **84**, 8195 (1987).
5. M. Prentky, C. B. Wollheim, P. D. Lew, *J. Biol. Chem.* **259**, 13777 (1984); J. B. Smith, L. Smith, B. L. Higgins, *ibid.* **260**, 11413 (1985).
6. H. Metzger *et al.*, *Annu. Rev. Immunol.* **4**, 419 (1986).
7. J. R. Cunha-Melo, N. M. Dean, J. D. Moyer, K. Maeyama, M. A. Beaven, *J. Biol. Chem.* **262**, 11455 (1987); V. S. Pribluda and H. Metzger, *ibid.*, p. 11449.
8. M. A. Beaven *et al.*, *ibid.* **259**, 7129 (1984); F. C. Mohr and C. Fewtrell, *ibid.* **262**, 10638 (1987); R. F. Stump, J. M. Oliver, E. J. Cragoe, Jr., G. G. Deanin, *J. Immunol.* **139**, 881 (1987).
9. E. L. Barsumian, C. Isersky, M. G. Petrino, R. P. Siraganian, *Eur. J. Immunol.* **11**, 317 (1981).
10. J. D. Taurog, C. Fewtrell, E. L. Becker, *J. Immunol.* **122**, 2150 (1979).
11. G. Grynkiewicz, M. Poenie, R. Y. Tsien, *J. Biol. Chem.* **260**, 3440 (1985).
12. Some Ca^{2+} leaked out of the IP_3-sensitive store of the permeabilized cells under these experimental conditions. The stores are not maximally loaded. In the presence of ATP and Mg^{2+} (which power the refilling of the IP_3-sensitive store), five to eight times as much Ca^{2+} can be released by addition of saturating amounts of IP_3.
13. In these experiments, fura-2 is the principal Ca^{2+} buffer as well as the Ca^{2+} indicator (T. Meyer, T. Wensel, L. Stryer, manuscript in preparation).
14. M. Prentky, C. B. Wollheim, P. D. Lew, *J. Biol. Chem.* **259**, 13777 (1984); J. B. Parys, H. De-Smedt, P. Vandenberghe, R. Borghraef, *Cell Calcium* **6**, 413 (1985); C. Heilmann, C. Spamer, W. Gerok, *J. Biol. Chem.* **260**, 788 (1985).
15. F. C. Mohr and C. Fewtrell, *J. Cell Biol.* **104**, 783 (1987).
16. C. P. Downes, M. C. Mussat, R. H. Michell, *Biochem. J.* **203**, 169 (1982); T. Y. Connolly, T. E. Bross, P. W. Majerus, *J. Biol. Chem.* **260**, 7868 (1985); T. Meyer, unpublished data.
17. D. Holowka, unpublished data.
18. The RBL cells studied here, like Syrian hamster insulinoma cells [S. K. Joseph, R. J. Williams, B. E. Corkey, F. M. Mataschinsky, J. R. Williamson, *J. Biol. Chem.* **259**, 12952 (1984)], are responsive to very low (nanomolar) concentrations of IP_3. Most other cells require a much higher IP_3 level for Ca^{2+} release. The differences in apparent IP_3 sensitivity may be due to differences in phosphatase and Ca^{2+}-adenosinetriphosphatase pump activities.
19. No cooperativity was observed in a study of the dependence of the rate of Ca^{2+} release on IP_3 concentration in permeabilized hepatocytes [J. R. Williamson, A. P. Thomas, S. K. Joseph, in *Inositol and Phosphoinositides, Metaholism and Regulation*, J. E. Bleasdale, J. Eichberg, G. Hauser, Eds. (Humana Press, Clifton, NJ, 1985), pp. 423–433]. The experimental conditions of Williamson *et al.* differed from ours in that ATP and Mg^{2+} were present, which may have increased hydrolysis of IP_3 and pumping of Ca^{2+} back into the IP_3-sensitive store.
20. A. Fabiato, *Am. J. Physiol.* **245**, 1 (1983).
21. Because $(k_- + k_+L) = k_-(1 + L/K_d)$ and equilibration is reached in less than 4 seconds for $L/K_d << 1$, k_- must be greater than 0.25 sec^{-1}. For the IP_3 receptor in brain, the apparent K_d is 40 nM and k_- is greater than 0.02 sec^{-1} [Worley *et al.* (*4*)].
22. J. W. Walker, A. V. Somlyo, Y. E. Goldman, A. P. Somlyo, D. R. Trentham, *Nature* **327**, 249 (1986).
23. N. M. Woods, K. S. R. Cuthbertson, P. H. Cobbold, *ibid.* **319**, 600 (1986); E. Neher and W. Almers, *EMBO J.* **5**, 51 (1986); K. S. R. Cuthbertson and P. H. Cobbold, *Nature* **316**, 541 (1985).
24. T. Meyer and L. Stryer, manuscript in preparation.
25. A. Brisson and P. N. T. Unwin, *Nature* **315**, 474 (1985); P. N. T. Unwin and P. Ennis, *ibid.* **307**, 609 (1984). A recent study [S. Supattapone, P. F. Worley, J. M. Baraban, S. H. Snyder, *J. Biol. Chem.* **263**, 1530 (1988)] shows that an IP_3 receptor from rat cerebellar membranes is multimeric. The mass of

the receptor under nondenaturing conditions is estimated to be 1000 kD, about four times the apparent mass of the dissociated chains under denaturing conditions.

26. Supported by grants from NIH (GM24032 and GM30387 to L.S. and AI22449 to D.H.). T.M. was a Swiss National Science Foundation Fellow. We thank B. Baird for stimulating discussions, T. Wensel for the Ca^{2+} chelating column, and P. Majerus for inositol 1:2-cyclic 4,5-trisphosphate.

2 February 1988; accepted 1 April 1988

ADP-Ribosyltransferase Activity of Pertussis Toxin and Immunomodulation by *Bordetella pertussis*

W. J. BLACK,* J. J. MUNOZ, M. G. PEACOCK, P. A. SCHAD, J. L. COWELL, J. J. BURCHALL, M. LIM, A. KENT, L. STEINMAN, S. FALKOW

Pertussis toxin is produced by the causative agent of whooping cough, *Bordetella pertussis*, and is an adenosine diphosphate (ADP)–ribosyltransferase capable of covalently modifying and thereby inactivating many eukaryotic G proteins involved in cellular metabolism. The toxin is a principal determinant of virulence in whooping cough and is a primary candidate for an acellular pertussis vaccine, yet it is unclear whether the ADP-ribosyltransferase activity is required for both pathogenic and immunoprotective activities. A *B. pertussis* strain that produced an assembled pertussis holotoxin with only 1 percent of the ADP-ribosyltransferase activity of the native toxin was constructed and was found to be deficient in pathogenic activities associated with *B. pertussis* including induction of leukocytosis, potentiation of anaphylaxis, and stimulation of histamine sensitivity. Moreover, this mutant strain failed to function as an adjuvant and was less effective in protecting mice from intracerebral challenge infection. These data suggest that the ADP-ribosyltransferase activity is necessary for both pathogenicity and optimum immunoprotection. These findings bear directly on the design of a nontoxic pertussis vaccine.

PERTUSSIS TOXIN IS THE PRIMARY determinant of virulence produced by *Bordetella pertussis* in whooping cough (*1–3*). Aspects of the systemic pathology of the disease, including lymphocytosis and hypoglycemia, can be reproduced in laboratory animals with purified toxin alone (*4*). The toxin is composed of five dissimilar polypeptides that can be divided into two functional subunits (*5*); an "A" monomer, S1, mediates adenosine diphosphate (ADP)–ribosylation of host G proteins (*6*), and a "B" oligomer, composed of four different polypeptides, designated S2 through S5, mediates binding of the toxin to host tissue (*7*). Two molecular mechanisms of pathogenesis have been proposed for pertussis toxin. The first is the ADP-ribosylation and concomitant inactivation of host G proteins involved in normal eukaryotic cell metabolism (*6*). The second mechanism is the lectin-like binding of the B oligomer to eukaryotic cells (*7*), which has been proposed to act mitogenically to cause the lymphocytosis and other immunomodulatory activities mediated by pertussis toxin (*8*).

Pertussis toxin is also found in, and is considered to be a primary protective component of, both the traditional whole-cell (*2, 9*) and the newer acellular (*10*) formulations of the pertussis vaccine. However, there is speculation that active toxin present in the vaccines may cause certain rare but serious vaccination sequelae including hypotonic, hyporesponsive syndrome, convulsions, and encephalopathy (*11*). Recent efforts to clone the toxin genes (*12*) are in part predicated on the proposition that an enzymatically inactive version of the toxin molecule produced by modified toxin genes might serve as a valuable component in a defined vaccine. We were interested in determining the contribution of the ADP-ribosyltransferase activity to pathogenesis and immunoprotection and so constructed *B. pertussis* strains with defined mutations in the toxin genes. These genes were assayed for the induction of leukocytosis (*4, 13*), the potentiation of anaphylaxis (*4, 14, 15*), and the stimulation of histamine sensitivity (*4*). We also examined the capacity of the strains to serve as adjuvants (*4*) and their immunoprotective activity against experimental *B. pertussis* infection in mice (*16*).

A *B. pertussis* strain with a nonpolar mutation that altered the primary structure of the pertussis toxin S1 or ADP-ribosyltransferase subunit was constructed by in vitro linker scanning mutagenesis (*17*), followed by allelic exchange (*18, 19*) of the mutation into the *B. pertussis* chromosome. This mutation, *ptx*A3201, introduced a 12-bp insertion at the Sal I restriction site of the S1 gene (Fig. 1), maintaining the reading frame integrity and introducing four novel codons, for Val-Asp-Gly-Ser, between Tyr^{141} and Val^{142} (*12*). We chose this site for modification because of its proximity to Glu^{140}; Collier and co-workers have shown that for each of two other ADP-ribosyltransferase toxins, diphtheria toxin and pseudomonas exopro-

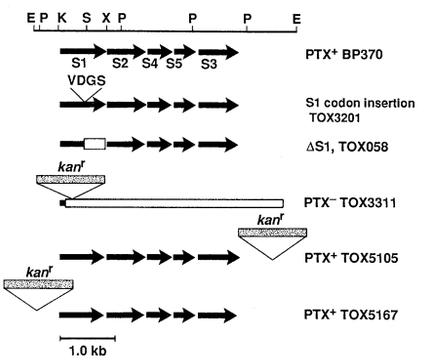

Fig. 1. Pertussis toxin operon mutations. Defined mutations in the pertussis toxin operon were constructed in vitro by means of standard recombinant DNA technology (*30*) and introduced into the chromosome of *B. pertussis* strain BP370 (*18*) by allelic exchange (*18, 19*). The parental *B. pertussis* strain, PTX+, BP370, contains a polycistronic arrangement of the genes for the five toxin polypeptide subunits (*12, 18*). The S1 codon insertion derivative, TOX3201, contains a 12-bp insertion, GACGGATCCGTC, at the Sal I site in the S1 gene, introducing the amino acids Val-Asp-Gly-Ser into the S1 polypeptide between Tyr^{141} and Val^{142} (*12*). The ΔS1 derivative, TOX058, contains a deletion of the 3′ half of the S1 gene, from the Sal I site to the Xba I site, fusing the S1 codon for Asp^{143} to the stop codon in the Xba I site. The construction of TOX3201 (*19*) and TOX058 (*27*) is described in greater detail elsewhere. TOX3201 was previously designated BP370*ptx*-3201 (*19*). The PTX− derivative, TOX3311, has a deletion extending from about 200 bp inside the 5′ end of the S1 gene down through about 1100 bp 3′ of the S3 gene, and a *kan*r gene (*26*) ligated into the breach (*18*). The PTX+, TOX5105 derivative has an insertion of the *kan*r gene about 800 bp 3′ of the toxin structural genes (*18*). The PTX+, TOX5167 derivative has an insertion of the *kan*r gene about 400 bp 5′ of the toxin structural genes (*18*).

W. J. Black and S. Falkow, Department of Medical Microbiology, Stanford University, Stanford, CA 94305.
J. J. Munoz and M. G. Peacock, Laboratory of Pathobiology, NIAID Rocky Mountain Laboratories, Hamilton, MT 59840.
P. A. Schad and J. L. Cowell, Department of Bacteriology, Praxis Biologics, Inc., Rochester, NY 14623.
J. J. Burchall, Burroughs Wellcome Company, Research Triangle Park, NC 27514.
M. Lim, A. Kent, L. Steinman, Department of Pediatrics, Stanford University, Stanford, CA 94305.

*To whom correspondence should be addressed at Department of Microbiology, Emory University School of Medicine, Atlanta, GA 30322.